Fabrication of porous carbon nitride foams/acrylic resin composites for efficient oil and organic solvents capture

Xiaohai Bu, Yi Lu, Shengwang Chen, Dongxian Li, Zewu Zhang, Ping Qian

PII: S1385-8947(18)31562-6
DOI: https://doi.org/10.1016/j.cej.2018.08.088
Reference: CEJ 19702

To appear in: *Chemical Engineering Journal*

Received Date: 4 May 2018
Revised Date: 8 August 2018
Accepted Date: 13 August 2018

Please cite this article as: X. Bu, Y. Lu, S. Chen, D. Li, Z. Zhang, P. Qian, Fabrication of porous carbon nitride foams/acrylic resin composites for efficient oil and organic solvents capture, *Chemical Engineering Journal* (2018), doi: https://doi.org/10.1016/j.cej.2018.08.088

Fabrication of porous carbon nitride foams/acrylic resin composites for efficient oil and organic solvents capture

Xiaohai Bu[a,b*], Yi Lu[b], Shengwang Chen[b], Dongxian Li[b], Zewu Zhang[a,b*], Ping Qian[c]

[a] Jiangsu Key Laboratory of Advanced Structural Materials and Application Technology, Nanjing, 211167, China

[b] School of Materials Science and Engineering, Nanjing Institute of Technology, Nanjing, 211167, China

[c] Jiangsu Suqing Water Treatment Engineering Group, Jiangyin, 214419, China

* Corresponding author: E-mail: xhbu@njit.edu.cn (X. Bu); zhangzw@njit.edu.cn (Z. Zhang)

Abstract

This article reported novel porous carbon nitride foams (CNFs)/acrylic resin composites for effective removal of oils and organic solvents from water. The composites were fabricated by a facile and low-cost method: carbonization of melamine-formaldehyde foams to form CNFs with hierarchal porosity and large specific surface area, following by hydrophobic treatment and in situ polymerization of acrylic monomers. A variety of characterizations including XPS, FT-IR, Raman spectra, XRD, and SEM had been performed to record the preparation process of the composites. The results demonstrated that the hydrophobic oil-absorbing resins were chemically attached onto the external surface of CNFs pores, which was beneficial for oil capture. The oil capture tests revealed that the composites had adsorption capacities of ~33.5 g g^{-1} to toluene and ~20.6 g g^{-1} to DMF, when 15wt% MCNFs were loaded. The excellent oil capture performances were owing to the combination of CNFs with oleophilic polymeric chains, which not only generated strong capillary and penetration interaction for oil absorption, but also provided large volume of space for oil storage. Despite of the high adsorption capacity, the composites also showed fast capture rate, good recyclability, and oil retention property, making them versatile candidates to satisfy the practical removal of oils and organic solvent from water.

Keywords: Carbon nitride foams, **Resin composite, Oil capture, Adsorption, Regeneration**

1. Introduction

With the boosting of industrialization, oil-polluted water has become a great challenge around the world due to the increasing industrial oily wastewater as well as frequent oil spill accidents. Oil pollution have caused severe environmental damages and economic lost in the past several decades. The development of oil-water separation technologies for the collection and elimination of oils or organic contaminants from polluted water is urgently needed. Nevertheless, traditional employed methods, including *in situ* burning[1], chemical dispersion[2], mechanical removal, bio-degradation[3], and physical absorption[4], commonly suffer from certain shortages, for instance, secondary air pollution, high operational costs, low efficiency, poor selectivity, etc. Hence, it is of practical significance to explore facile, low-cost and efficient approaches to resolve such environmental problems.

The use of oil-absorbing materials with excellent sorption selectivity and capacity are considered to be one of the most promising candidates in recent years[5-7]. Adsorbents such as activated carbon[8], fibers[9], aerogels[10], and resins[11] are widely studied and exploited due to their low density, chemical inertness, and large specific surface area. Amongst them, oil-absorbing resins mostly synthesized from oily organic monomers has been increasingly utilized. They are capable to create cross-linked three-dimensional (3D) networks which can immobilize the oils *via* van der Waals forces between the lipophilic groups and surrounding organic contaminants[12, 13]. After adsorption, the resins would swell but not dissolve in the oils, thus achieving the oil preservation purpose. In particular, the rapid absorption rate, considerable oil retention

capacity and excellent reusability of oil-absorbing resins are also proven to be indispensable for emergency pollution abatements [11, 14, 15]. To date, various polyolefin and polyacrylate copolymer have been demonstrated by researchers. Yuan et al.[16] prepared a cross-linked polyolefin terpolymer with outstanding oil capture ability (up to 45 times of the polymer weight) and fast adsorption kinetics, which was suitable for regular oil-refining processes. Du et al.[17] reported a macroporous St/BMA copolymer resin synthesized by suspension copolymerization and the resin exhibited a great performance of reuse and regeneration. Chen and coworkers[18] introduced 4.54 wt% of weakly coordinating ions into the styrene/butyl methacrylate/stearyl methacrylate copolymer networks and obtained a novel type of polyelectrolyte resin with a maximal oil absorbency of 37.86 g g^{-1} to CCl_4. Although remarkable achievements to improve the synthesis and properties of oil-absorbing resins have been made, the high cost, poor mechanical properties and complicated synthesis process of them are still critical factors that block their practical promotion. Innovative molecular designing of resins or hybridization with porous materials is indeed required to surmount these disadvantages.

Acrylic resin is a crosslinked polymer with 3D networks and possess various attractive properties in oil capture, including good selectivity, easy regeneration, and resistance to water. However, traditional acrylic resins still exhibit serval disadvantages, such as slow oil capture rate and low oil absorption capacity. Incorporation of designed hydrophobic acrylate units and decreasing the degree of crosslinking can improve the general structure of the resins which will result in enhanced oil capture properties.

Composites constructed by chemically attaching oil-absorbing resins onto the external surface of porous support pores are of special interests. Utilizing the porous materials as supporting skeleton, a certain amount of lipophilic polymers are introduced by *in situ* polymerization to form resin composites with considerable mechanical properties and chemical stability, as well as other unique properties[19, 20]. During the oil capture process, the hydrophobic and oleophilic polymeric chains drag oily molecules from water and absorb them into the inner pores by capillary and penetration interaction, while the void fraction of porous support provides large volume of space for oil storage. A variety of experimentally available materials with unique porosity including Al_2O_3[21], MnO_2[22], LDHs[23], CNTs[24], etc. have been reported as the functional fillers to form resin-based composites. However, these nano-/micrometer sized materials are always expensive, nondegradable, or difficult for large-scale production. Considering the important factors in practical cost, usage, and post-processing, advances in finding new porous fillers should be made.

Porous nitrogen doped carbon materials are typically lightweight, self-supported, chemically stable, and rich in activated sites, which hold great potential in a wide range of areas, especially in energy storage, catalyst supports, and absorbers[25-27]. The preparation of these materials can be mainly classified into three categories: (i) annealing of graphitized porous carbon materials in NH_3[28]; (ii) pyrolysis of nitrogen-containing polymers with the help of pore-forming templates[29]; (iii) direct carbonization of the nitrogen-containing polymer foams, for example, melamine-formaldehyde (MF) resin[30]. As a commercially available product, MF foams offer

many advantages, such as low-cost, low density, high scalability, large specific area as well as hierarchical porous structure. When MF foams are employed as the precursor for carbonization, the obtained CNFs offer unique open network with micrometer-sized pores and high nitrogen contents, which may be beneficial for the capture of oils[31, 32]. Importantly, the extensive binding sites in the CNFs framework can be simply modified with hydrophobic polymers, thus indicating great improvement in the oil absorbing rate and oil retention for oil-water separation.

In this paper, we firstly employ a facile and cost-effective strategy to the fabricate porous CNFs/acrylic resin composites, which exhibit excellent oils and organic solvents capture performance. The CNFs with a large specific area and unique hierarchical porosity are synthesized by a direct high-temperature carbonization route with MF foams as the precursor. Then, the CNFs are subsequently modified with hydrophobic coupling agents and copolymerized with selected acrylate monomers to introduce their hierarchical porosity into the resulting resin composites. Porosity and hydrophobicity of the as-obtained composites are demonstrated in the characterization results of morphology and contact angle analyses. Furthermore, the influence of the CNFs loading contents from 0 to 35wt% in composites on oil capture capacity are studied in detail. The results show remarkable oil absorbing properties for some common organic solvents and oils. Finally, regeneration experiments are performed to demonstrate the good reusability of the composites in order to meet the current needs in piratical applications.

2. Experimental Section

2.1. Materials

Butyl acrylate (BA), butyl methacrylate (BMA), N,N-methylene-bis-acrylamide (MBA) and benzoyl peroxide (BPO) were purchased from Sinopharm Chemical Reagent Co., Ltd. BPO was recrystallized using chloroform/methanol (1/1, v/v), dried at 60 °C, and stored in an amber bottle. Polyvinyl alcohol (PVA, DP=1700) and γ-methacryloxypropyl trimethoxysilane (KH-570) were obtained from Aladdin. MF foams was supplied by Sichuan Golden-Elephant Sincerity Chemical Co., Ltd. Engine and edible oils were purchased from the local market, Nanjing, China. All other regents (analytical grade) were used as received without further purification and deionized water was used for all the experiments.

2.2. Characterization

Fourier transform infrared (FT-IR) spectra were carried out on a Nicolet iS10 FT-IR spectrometer at room temperature using KBr pellets. The spectra were obtained at a 4 cm^{-1} resolution and recorded in the region of 4000-400 cm^{-1}. Raman spectra were recorded on a Renishaw inVia Raman Microscope with an excitation wavelength of 514 nm. XPS data were collected from Shimadzu Amicus X-ray photoelectron spectrometer. XRD patterns of the samples were tested using a Rigaku D/MAX-R with a copper target at 40 kV and 30 mA. The diffractograms were recorded in the range 5 ~ 70 ^{o} at the speed of 3 ^{o} min^{-1}. Scanning electron microscopy (SEM) images and energy dispersive spectra (EDS) were obtained on a S-4800 (Hitachi, Japan) field-emission scanning electron microscope. The EA results were obtained using an elemental analyzer

(Elementar Vario MACRO cube). The contact angles of samples were measured by a JY-82C video contact angle analyzer. For each sample, an average contact angle value was given according to five times tests on the different location of the sample. The Brunauer-Emmett-Teller (BET) surface area tests were recorded on a V-Sorb/2800TP nitrogen adsorption-desorption instrument operated at 77 K. The pore size distribution of the sample was determined by assuming cylindrical pore model *via* Barret-Joyner-Halender (BJH) method. The CNFs/acrylic resin composite with 15wt% MCNFs loading is taken as representative composite sample for FT-IR spectra, contact angles, surface area test and XRD measurements.

2.3. Preparation of porous CNFs

In a typical procedure, 30 g of MF foams was placed in a tube furnace under nitrogen environment and the temperature of the furnace was firstly increased to 150 °C in 1 h and maintained for 0.5 h. The temperature was sequentially increased to 600 °C at a heating rate of 10 °C min^{-1} and maintained at the desired temperature for 3h for complete carbonization, followed by natural cooling to room temperature. The product was washed with ethanol and dried under vacuum at 60 °C to obtain porous CNFs. Then, the as-synthesized CNFs was transferred into a 100mL Teflon vessel, in which 0.5 mL of concentrated HNO_3 was added previously. The Teflon vessel was sealed in an autoclave and reacted at 120 °C for 2 h and the oxidized CNFs (OCNFs) was washed with ethanol and dried under vacuum at 60 °C for 2 h.

2.4. Hydrophobic modification of porous CNFs

The OCNFs was further modified with a silane coupling agent, KH-570, to endow the

porous CNFs with hydrophobicity and provide the carbon-carbon double bonds for further graft polymerization of acrylic resin. The modification process is performed as follows: 10 g of as-prepared OCNFs, 3.6 g of KH-570 and 50 mL of toluene were mixed under high-intensity ultrasonication for 15 min at 30 °C. The mixture was then heated to 110 °C in the oil bath and refluxed for 12 h. The resulting KH-570 modified CNFs (MCNFs) was filtered, washed thoroughly with acetone and dried under vacuum at 80 °C for 24 h.

2.5. Fabrication of porous CNFs/acrylic resin composites

The acrylic resin composites were prepared by a suspension polymerization method. In a typical experiment, 2.4 g of PVA was firstly dissolved in 30 mL of deionized water and stirred at 90 °C until the solution became clear. The PVA aqueous solution was then cooled to room temperature naturally. A mixture containing a certain amount of MCNFs, 12 g of BA, 12 g of BMA, 0.3 g of MBA and 0.2 g of BPO were added into the solution under nitrogen atmosphere at 70 °C and reacted for 4 h. Finally, the as-obtained composite was collected, sequentially washed with deionized water and ethanol, and dried under vacuum at 60 °C for 24 h. The scheme of the composite preparation process is shown in Fig. 1, and a series of porous CNFs/acrylic resin composites with fixed amounts of CNFs were prepared through the above method, just changing the weight percentage of the loading MCNFs (0, 5wt%, 15wt%, 25wt%, and 35wt%, respectively) in the composites.

2.6. Oil capture experiment

The oil capture experiments were determined by a gravimetric method at room

temperature. Dried porous CNFs/acrylic resin composites were weighed beforehand and immersed into the various oils and organic solvents (toluene, CCl_4, edible oils, etc.). After 24 h, the composites were taken out from oils, drained for 3 min to remove excess oil, and then weighted immediately. The oil capture capacities of the samples were determined by weighing the samples before and after absorption, and calculated by the following formula:

$$Q = (G_1 - G_0)/G_0$$

where Q ($g \cdot g^{-1}$) is the oil capture capacity of the oil absorbents calculated as grams of oil per gram of composite, G_1 and G_0 (g) is the weight of the dry absorbents and wet oil immersed absorbents after draining, respectively. All oil capture capacities were measured three times, and an average value was finally given.

2.7. Regeneration experiment

In order to examine the reusability of the oil absorbents, the composites were firstly immersed in given oils for saturated absorption and then the composites were transferred to a mass of anhydrous ethanol to release the absorbed oil for 24 h. Finally, the composites were taken out and dried under vacuum at 60 °C for 12 h. The process of oil absorption-desorption test was repeated three times and the composites were weighed before and after oil absorption for each cycle.

3. Results and Discussion

3.1. Fabrication and characterization of CNFs/acrylic resin composites

Fig. 1 shows the synthetic strategy for the preparation of porous CNFs/acrylic resin composites. The high-temperature carbonization of MF foams to form CNFs offer open network with micrometer-sized pores and high nitrogen contents, thus offering abundant binding sites for the surface modification. As shown in Fig. S1 and Table S1, the EDS and EA results of the CNFs clearly indicates the CNFs are mainly constructed by carbon, nitrogen and oxygen elements, which exhibit a C : N atomic ratio of 1.3 : 1. XPS measurements are further performed to investigate the elemental composition and chemical states of C and N in the CNFs. As is shown in Fig. 2a, XPS spectrum for CNFs samples clearly show the incorporation of nitrogen atoms within the graphitic carbon. In Fig. 2b, the high-resolution C 1s spectra of the CNFs obtained by peak fitting shows three main peaks at 284.7 eV, 285.9 eV, and 287.5 eV corresponding to sp^2-hybridized graphitic carbon atoms (C-C/C=C), sp^2-hybridized carbon bonded with doped nitrogen (C=N), and sp^3-hybridized carbon bonded with doped nitrogen (C-N), respectively. This observation indicates the formation of C-N bonds in the graphitic carbon network during the pyrolysis process. Meanwhile, small signals at higher binding energy of C-O and C=O also reveals that most of the oxygen containing functional groups have been removed, and the graphitic carbon network are formed. The N 1s spectra of the CNFs in Fig. 2c can be fitted into three peaks at 398.4 eV, 399.5 eV, and 400.7 eV, which can be attributed to the pyridine-like, pyrrole-like, and graphitic nitrogen. The bonding configurations of N elements indicate that a large number of nitrogen atoms are incorporated into the graphene networks in the CNFs by forming five and six-membered aromatic rings[33]. All the above XPS results

demonstrate the successful synthesis of nitrogen rich CNFs through the annealing of MF foams under inert atmosphere.

In order to fabricate the acrylic resin composites using CNFs as porous fillers, the CNFs are further oxidized by nitric acid, hydrophobically modified by KH-570 and used as porous reinforcement in the preparation process. Raman spectroscopy is a direct and nondestructive method to estimate the chemical structures and determine the defects for carbon materials. The Raman spectra of CNFs, OCNFs and MCNFs are collected at an excitation wavelength of 514 nm under ambient conditions and shown in Fig. 3. For the three samples, the remarkable peaks at 1359 cm^{-1} (D band) and 1579 cm^{-1} (G band) which are respectively assigned to the A_{1g} breathing mode of disordered graphite and the E_{2g} stretching mode of graphite structure are obviously observed, demonstrating the that the present thermal annealing process results in carbon materials. Meanwhile, no characteristic peaks at 950~1000 cm^{-1} corresponded to the ring breathing vibration of the triazinyl rings in melamine can not be found, indicating the complete graphitization of MF foams[32]. The I_D/I_G ratios of CNFs, OCNFs and MCNFs are calculated to be 1.03, 1.16, and 1.19. It can be inferred that the CNFs and related materials exhibit high concentrations of defect sites due to the abundant doped nitrogen atoms in the graphite structure.

Infrared spectroscopy is a useful method for detecting the changes of chemical bonds. The FT-IR spectra of MF foams, CNFs, OCNFs, MCNFs and CNFs/acrylic resin composite are shown in Fig. 4. The MF foams shows the typical characteristic absorption peaks centered at 3300 cm^{-1}, 1485 cm^{-1}, and 1336 cm^{-1} in Fig. 4a, which are

corresponded to the stretching vibration of N-H, O-H, C=N and C-N-C bonds of triazine rings, respectively. After annealing at 600 °C for 3h, all the absorption peaks of MF foams disappear, apart from a very weak absorption at around 1700 cm^{-1} in Fig. 4b. From these observations, it can be deduced that the triazine rings and other formed chemical bonds have been completely decomposed through pyrolysis and nitrogen rich CNFs are formed. In Fig. 4c, the obvious broad absorption peaks centered at 3480 cm^{-1} and 1720 cm^{-1}, which may be dedicated to the hydroxyl and carbonyl groups, confirm the surface oxidization of the CNFs by nitric acid. When the OCNFs are hydrophobically modified with KH-570, the absorption peaks of methyl and methylene groups at 2960 cm^{-1}, 2920 cm^{-1}, and 2853 cm^{-1} in the vinyl containing silane coupling agent molecular can be observed in Fig. 4d. For the CNFs/acrylic resin composite, strong absorption peaks corresponding to a typical cross-linked acrylate copolymer can be found in Fig. 4e, demonstrating the successful copolymerization of the monomers in the presence of MCNFs and formation of the CNFs/acrylic resin composite.

The phase structure is investigated by means of powder XRD technique, and the diffraction patterns of as-prepared samples are displayed in Fig. 5. The broad diffraction peak centered at $2\theta = 26.7^{o}$ of CNFs, OCNFs and MCNFs may be assigned to the (002) crystal planes of graphite-like stacking structure of the aromatic CN units, indicating that the pyrolysis treatment lead to the graphitization of MF foams to CNFs[34]. Meanwhile, it can be observed that CNFs, OCNFs and MCNFs have similar diffraction pattern characteristics, suggesting that surface oxidization and modification have few effects on the crystalline structures of CNFs. With regard to the CNFs/acrylic

resin composites, an amorphous region around 2θ = 18.8 º is additionally observed compared to that of CNFs, which can be assigned to the characteristic amorphous structure of acrylic resin in Fig. S2. The XRD patterns further suggest that the successful fabrication of the composites, in good agreement with the FT-IR analysis.

With regard to adsorbing materials, special surface area and porosity have great influence on their oil capture capacity and absorption rate. The N_2 adsorption-desorption isotherm and corresponding pore size distribution for CNFs are shown in Fig. 6a. The isotherm curve of CNFs exhibits the typical adsorption hysteresis that belongs to type I isotherm curves, indicating the presence of large amount of micro- and mesopores. The pore size distribution is measured according to the BJH model which reveals that the majority of the pores in the CNFs have size mostly around 0.6 nm and 4.5 nm. Meanwhile, the sample is also found to possess a relative large BET specific surface area of about 452.48 m^2 g^{-1}, which is ascribed to the coexistence of micro- and mesopores. The unique porous characteristic may be resulted from escape of various gases (e.g. NH_3, H_2O, and N_2) originated from decomposition of oxygen and nitrogen groups at high temperature[31, 35]. The formation of interconnected pores in the CN frameworks will be extremely useful for efficient mass transport during oil absorption. For the composite, N_2 adsorption-desorption isotherm is shown in Fig. 6b. Different from the isotherm of CNFs, the sample shows a type-IV isotherm with an upward deviation in the relative pressure range of 0.6-0.9, indicating the presence of mesoporous structures in the composite. The pore size distribution in the inset demonstrates that the composite mainly exhibits a pore diameter of 2~48 nm. The

disappearance of the micropores is because of the occupancy of the polymer chains. The broaden mesopore distribution may come from the pores created by the cross-linked acrylic resins grafted at the inner pore surface. The specific surface area of the composite is about 28.56 m^2 g^{-1}, which is larger than many acrylic resins and their composites. However, it is notable that the quantity of adsorbed N_2 and corresponded specific area of the composite are lower compared to pristine CNFs. The phenomena may be owing to a degree of pore breakage during the chemical treatment and the resin filling in the pores. From this, it is not hard to deduce that the micro- and mesopores of the CNFs in the composites are blocked to a great extent. Hence, the oil adsorption of the composites is mainly dependent on the macropores, which is different from the pristine CNFs.

The morphology and pore structure of the CNFs and CNFs/acrylic resin composites are analyzed by field emission scanning electron microscope and the results are shown in Fig. 7 and Fig. S3. From SEM images of Fig. 7a and b, it can be seen that the CNFs display a 3D cellular network structure composed of interconnected pore with a diameter range of 60~200 μm, while the thickness of the skeleton is about 10 μm. As presented in the BET results, it is easy to concluded that a hierarchical porous structure including micropores, mesopores and micrometer-sized pores are formed in the CNFs. When the CNFs participate in polymerization of acrylate monomers, more smooth and apparent surface of the skeleton are observed in Fig. 7c and d, indicating the successful grafting of the organic polymers on to the internal surface of CNFs. The composites also consist of a great number of well-organized pores of ca. 30~100 μm, which

demonstrate that no structural damage or blockage appear during the *in situ* polymerization of acrylate monomers. This observation further affirm that the preparation strategy completely preserves the open-framework structure of CNFs to the composites. Different from pristine oil-absorbing resins, the unique micrometer-sized porosity of CNFs/acrylic resin composites may provide more volume space and channels to effectively improve the oil storage capacity and reduce the mass transfer resistance.

3.2. Oil capture capacity of composites

Wettability of the materials to water or oils is a key parameter for oil capture. The Contact angle tests are used to record the hydrophobic properties of the as-prepared samples. The measurements are performed by compressing the samples on a glass slide flowed with a sessile drop method with water and toluene. The water wettability of CNF, OCNF, and MCNFs are shown in Fig S4. CNFs exhibits a water contact angle of 120.09 ° which may be derived from the hydrophobicity of the graphitic carbon networks. The water contact angles of OCNFs and MCNFs are 103.23 ° and 127.36 °, indicating the successful surface oxidization and hydrophilic modification of CNFs. Fig. 8 shows the water and toluene contact angle profiles of the CNFs/acrylic resin composites. In Fig. 8a and b, the composite exhibits a hydrophobic character with a stable water contact angle of 142.27°, inferring that the presence of hydrophobic acrylic resin chains grafting on the surface of CNTs. Besides, with the increasing time of contact with the composites, the water droplet keeps spherical shape and does no sink into the composites. When toluene droplet is dropped onto the surface of the composites in Fig.

8c and d, the contact angle is around 30.81° within ~0.062 s. After that time, the droplet quickly spread out and sink into the tested sample, suggesting the excellent lipophilicity of the composites. The opposite wettability between water and toluene further confirm the potential organic solvents and oils capture capacity of the as-prepared composites. As mentioned above, CNFs acted as a porous framework may introduce the organic acrylic resins with tremendous three-dimensional networks and significantly enhance their oil capture capacities. Hence, it is necessary to discuss the effect of CNFs loading contents on their oil capacities. The oil capture amount *Q* for corresponding composites with different MCNFs loading contents (0, 5wt%, 15wt%, 25wt%, and 35wt%) were measured with three common organic solvents: toluene, chloroform, and DMF. As shown in Fig. 9, the incorporation of MCNFs may drastically increase the absorbencies for organic solvents for all the solvents, and the *Q* values are depending on the loading contents of MCNFs. For toluene, pristine acrylic resin only has a capture capacity of ~11.7 g g^{-1}. It is obvious that the oil capture capacities increase with the increasing MCNFs content in the composites. When the MCNFs loading content is set to 15 wt%, the composite has a maximum capture capacity of ~33.5 g g^{-1}, which is about 3 times of pristine acrylic resin. The improvement in oil capture capacity is undoubtedly owe to the addition of MCNFs which endows the composites with 3D network structure and hierarchical porosity. Besides, the capture capacities show an obvious decrease tendency with the increasing MCNFs loading content above 15 wt%. The dependency of oil capture capacity on the MCNFs loading contents can be explained as follows: Lower MCNFs loading may cause the over-grafting of the resins in the void of CNFs

frameworks which limit the swelling of resins and decrease the oil storage volume; Higher MCNFs loading may not only decrease the hydrophobicity and crosslinking degree of the polymer, but also result in heterogeneous distribution of polymers in the interior pores of CNFs. For low-density organics, all these can significantly weaken the oil swelling effect and decrease the oil capture capacity so that an optimized MCNFs loading is indeed required. The chloroform capture experiments also show a similar oil absorption property with the increasing MCNFs loading contents, and the maximum capture capacity is up to ~32.7 g g^{-1}. DMF is an organic solvent with a high boiling point and strong carcinogenicity which has been commonly used in industry. DMF capture experiments are further performed and the results show that the composites have relatively high capture capacities compared with some reported materials listed in Table S2. The capture capacity of the composite loaded with 15wt% MCNFs is measured to be ~20.6 g g^{-1} and the value slightly decreases as the loading content increases above 15wt%. These phenomena may possibly attribute to efficient diffusion of the DMF molecules in the hierarchical pores and the intermolecular interaction with active sites of the nitrogen rich 3D frameworks.

In order to systematically investigate the oil capture capacities of the CNFs/acrylic resin composites, samples are immersed in oils or organic solvents without water for 24 h and the maximum absorption capacities were determined by mass change. Because of the prominent capture capacity of the composite with a MCNFs loading of 15wt%, it is chosen as the optimum sample for the experiments. Nine kinds of frequently encountered organic solvents and oils, for instance, acetone, xylene, CCl_4, ethyl acetate,

N-methyl pyrrolidone (NMP), benzene, engine oil, edible oil, and THF are tested to evaluate the capture capacities of the composites. In general, the capture capacities of the composite shown in Fig. 11 are 5.1~40.9 times its own weight, which shows high absorbency for the measured oils and organic solvents. Moreover, it can be seen that the composite has a higher capture capacity in less and nonpolar organic solvents (i.e. xylene, CCl_4, and benzene), while a lower capture capacity in some polar organic solvents. Nevertheless, the capture performance of the composite for edible oil and engine oil is much lower than that of organic solvents, which may be explained by the fact that the self-swelling property of resin composite are more preferably for small molecule solvents[21, 22].

Based on the hierarchical porosity, interconnected 3D framework and strong lipophilicity of the as-obtained CNFs/acrylic resin composites, they should be ideal candidates for the fast elimination of oily pollutants. The typical capture processes for toluene (labeled with Sudan III dye) on the surface of water at different time intervals are vividly displayed in Fig. 12 and Fig. S5. A piece of the composite (~0.1 g) is immersed into the mixture with 2 mL of toluene floating on the surface of water in a sealed bottle. The floated red organics rapidly transfer from the water surface to the composite without leaving a trace, and the composite piece swells within about 5 minutes, implying the fast capture rate of the composites. when the composite is taken out, the majority of absorbed toluene are firmly stored in the abundant hierarchical pores of the composite, which further confirms the high capture capacity of the composites. Therefore, it is not difficult to speculate that the composites can also

efficiently and quickly clean up the other organic pollutants on water surface to alleviate the environmental problem.

3.3. Regeneration of composites

The recyclability of the oil-absorbents and the recoverability of pollutants are important criteria for practical oil cleanup applications. The regeneration of the composites is researched by measuring the oil capture capacities of three different oils or organic solvents. The composites are immersed in the oils or organic solvents for saturated absorption and then desorb them in a large amount of ethanol for next absorption test. The capture capacities of the composites after four repeated absorption-desorption cycles for toluene, DMF and edible oil are illustrated in Fig. 13. It is desirable to note that no obvious change in capture capacities is found after for absorption-desorption cycles. After four cycles, the capture capacity for toluene is 31.3 g g^{-1}, which decrease less than 1% of the value in the first capture. The regeneration results for DMF and edible oil also shows a similar change in capture capacities. The excellent recyclability can be likely due to the stable hierarchical porous structure of the composites during the whole process. In addition, the mass loss of the regenerated composites is also calculated to be lower than 3%, resulting in good oil retention capacities. This is not only ascribed to the mild desorption procedure without severe disruption of the materials, but also ascribed to the robust 3D framework of CNFs and the relatively strong chemical interaction between the porous fillers and polymers. According to the different oil capture capacities and easy regeneration of the acrylate CNFs/acrylic resin composites, these materials still show unique advantages on oil absorption selectivity,

recyclability and oil retention property due to the incorporation of acrylic resin, despite their lower capture capacities compared to neat CNFs and MOF-decorated CNFs in previous reports. Judging from the above viewpoints, the composites clearly show admirable potential when used as oil-absorbents piratically.

4. Conclusions

In summary, a low-cost and efficient fabrication strategy for CNFs-containing composites was successfully established by combining the direct carbonization of MF foams and *in situ* polymerization of acrylic resins. The CNFs derived from MF foams contained a large amount of nitrogen atoms and defect sites in their graphite-like 3D networks. Most importantly, the CNFs possessed unique hierarchical porous structure composed of micrometer-sized pores (60~200 μm), mesopores (~4.5 nm) and micropores (~0.6 nm) and large BET specific surface area of 452.48 m^2 g^{-1}. The obtained composites with excellent hydrophobicity and lipophilicity showed the optimum capture capacities to oil and organic solvents when 15wt% MCNFs were loaded. The capture capacity for toluene and DMF could reach ~33.5 g g^{-1} and ~20.6 g g^{-1}, respectively, which was higher to many reported oil-absorbing materials. While having high oil capture capacity, the composites also exhibited rapid absorption rate, great recyclability, and oil retention property. Therefore, we can predict that the CNFs/acrylic resin composites in this work will undoubtedly be an efficient and durable oil capture material for the practical oil/water separation.

Acknowledgments

The authors are financially supported by the National Nature Science Foundation of China (61705101, 21603101), Natural Science Foundation of Jiangsu (BK20160774), Natural Science Fund for Colleges and Universities in Jiangsu Province (17KJB430017), Opening Project of Jiangsu Key Laboratory of Advanced Structural Materials and Application Technology (ASMA201604), Science Foundation of Nanjing Institute of Technology (YKJ201604), the Outstanding Scientific and Technological Innovation Team in Colleges and Universities of Jiangsu Province and Jiangsu Students' Innovation and Entrepreneurship Training Program (201711276010Z).

References

[1] A. B. Nordvik, M. A. Champ, K. R. Bitting, Estimating time windows for burning oil at sea: Processes and factors, Spill Sci. Technol. Bull. 8 (2003) 347-359.

[2] Z. Li, K. Lee, T. King, M. C. Boufadel, A. D. Venosa, Effects of temperature and wave conditions on chemical dispersion efficacy of heavy fuel oil in an experimental flow-through wave tank, Mar. Pollut. Bull. 60 (2010) 1550-1559.

[3] S. Cappello, A. Volta, S. Santisi, C. Morici, G. Mancini, P. Quatrini, M. Genovese, M. M. Yakimov, M. Torregrossa, Oil-degrading bacteria from a membrane bioreactor (BF-MBR) system for treatment of saline oily waste: Isolation, identification and characterization of the biotechnological potential, Int. Biodeterior. Biodegrad. 110 (2016) 235-244.

[4] B. Li, X. Liu, X. Zhang, J. Zou, W. Chai, Y. Lou, Rapid adsorption for oil using superhydrophobic and superoleophilic polyurethane sponge, J. Chem. Technol. Biotechnol. 90 (2015) 2106-2112.

[5] M. O. Adebajo, R. L. Frost, J. T. Kloprogge, O. Carmody, S. Kokot, Porous materials for oil spill cleanup: A review of synthesis and absorbing properties, J. Porous Mater. 10 (2003) 159-170.

[6] W. Deng, M. Long, X. Miao, N. Wen, W. Deng, Eco-friendly preparation of robust superhydrophobic $Cu(OH)_2$ coating for self-cleaning, oil-water separation and oil sorption, Surf. Coat. Technol. 325 (2017) 14-21.

[7] C. T. Liu, P. K. Su, C. C. Hu, J. Y. Lai, Y. L. Liu, Surface modification of porous substrates for oil/water separation using crosslinkable polybenzoxazine as an agent, J. Membr. Sci. 546 (2018) 100-109.

[8] A. L. Ahmad, S. Sumathi, B. H. Hameed, Residual oil and suspended solid removal using natural adsorbents chitosan, bentonite and activated carbon: A comparative study, Chem. Eng. J. 108 (2005) 179-185.

[9] H. Zhu, S. Qiu, W. Jiang, D. Wu, C. Zhang, Evaluation of electrospun polyvinyl chloride/polystyrene fibers as sorbent materials for oil spill cleanup, Environ. Sci. Technol. 45 (2011) 4527-4531.

[10] Y. Yang, Z. Tong, T. Ngai, C. Wang, Nitrogen-rich and fire-resistant carbon aerogels for the removal of oil contaminants from water, ACS Appl. Mater. Interfaces 6 (2014) 6351-6360.

[11] M. H. Zhou, C. S. Ha, W. J. Cho, Synthesis and properties of high oil- absorptive

network polymer 4- tert- butylstyrene-SBR-divinylbenzene, J. Appl. Polym. Sci. 81 (2001) 1277-1285.

[12] H. H. Sokker, N. M. El-Sawy, M. A. Hassan, B. E. El-Anadouli, Adsorption of crude oil from aqueous solution by hydrogel of chitosan based polyacrylamide prepared by radiation induced graft polymerization, J. Hazard. Mater. 190 (2011) 359-365.

[13] A. Li, H. X. Sun, D. Z. Tan, W. J. Fan, S. H. Wen, X. J. Qing, G. X. Li, S. Y. Li, W. Q. Deng, Superhydrophobic conjugated microporous polymers for separation and adsorption, Energy Environ. Sci. 4 (2011) 2062-2065.

[14] P. Fang, P. Mao, J. Chen, Y. Du, X. Hou, Synthesis and properties of a ternary polyacrylate copolymer resin for the absorption of oil spills, J. Appl. Polym. Sci. 131 (2014) 40180 .

[15] C. S. Ye, H. X. Wang, G. Q. Huang, T. Qiu, Adsorption and desorption of DMF on macroporous resin NKA-II in the fixed bed, Chem. Eng. Res. Des. 91 (2013) 2713-2720.

[16] X. Yuan, T. C. M. Chung, Novel solution to oil spill recovery: using thermodegradable polyolefin oil superabsorbent polymer (Oil-SAP), Energy Fuels 26 (2012) 4896-4902.

[17] Y. Du, P. Fang, J. Chen, X. Hou, Synthesis of reusable macroporous St/BMA copolymer resin and its absorbency to organic solvent and oil, Polym. Adv. Technol. 27 (2016) 393-403.

[18] J. Chen, P. Fang, Y. Du, X. Hou, Synthesis and properties of lipophilic polyelectrolyte styrene/butyl methacrylate/stearyl methacrylate resin as absorbent

materials for organic solvents and oils, Colloid Polym. Sci. 294 (2016) 119-125.

[19] Z. Abbasi, E. Shamsaei, X. Y. Fang, B. Ladewig, H. Wang, Simple fabrication of zeolitic imidazolate framework ZIF-8/polymer composite beads by phase inversion method for efficient oil sorption, J. Colloid Interface Sci. 493 (2017) 150-161.

[20] L. Qi, H. ShamsiJazeyi, G. Ruan, J.A. Mann, Y. H. Lin, C. Song, Y. Ma, L. Wang, J. M. Tour, G. J. Hirasaki, R. Verduzco, Segregation of amphiphilic polymer-coated nanoparticles to bicontinuous oil/water microemulsion phases, Energy Fuels 31 (2017) 1339-1346.

[21] X. Yue, T. Zhang, D. Yang, F. Qiu, J. Rong, J. Xu, J. Fang, The synthesis of hierarchical porous Al_2O_3/acrylic resin composites as durable, efficient and recyclable absorbents for oil/water separation, Chem. Eng. J. 309 (2017) 522-531.

[22] C. Zhang, D. Yang, T. Zhang, F. Qiu, Y. Dai, J. Xu, Z. Jing, Synthesis of MnO_2/poly(n-butylacrylate-co-butyl methacrylate-co-methyl methacrylate) hybrid resins for efficient oils and organic solvents absorption, J.Clean. Prod. 148 (2017) 398-406.

[23] Y. Wang, Q. Li, L. Bo, X. Wang, T. Zhang, S. Li, P. Ren, G. Wei, Synthesis and oil absorption of biomorphic MgAl layered double oxide/acrylic ester resin by suspension polymerization, Chem. Eng. J. 284 (2016) 989-994.

[24] J. Rong, X. Rong, F. Qiu, X. Zhu, J. Pan, T. Zhang, D. Yang, Facile preparation of glucose functionalized multi-wall carbon nanotubes and its application for the removal of cationic pollutants, Mater. Lett. 183 (2016) 9-13.

[25] L. F. Chen, Y. Lu, L. Yu, X. W. Lou, Designed formation of hollow particle-based

nitrogen-doped carbon nanofibers for high-performance supercapacitors, Energy Environ. Sci. 10 (2017) 1777-1783.

[26] N. Tachibana, S. Ikeda, Y. Yukawa, M. Kawaguchi, Highly porous nitrogen-doped carbon nanoparticles synthesized via simple thermal treatment and their electrocatalytic activity for oxygen reduction reaction, Carbon 115 (2017) 515-525.

[27] X. Li, Z. Y. Sui, Y. N. Sun, P. W. Xiao, X. Y. Wang, B. H. Han, Polyaniline-derived hierarchically porous nitrogen-doped carbons as gas adsorbents for carbon dioxide uptake, Microporous Mesoporous Mater. 257 (2018) 85-91.

[28] X. Wang, X. Li, L. Zhang, Y. Yoon, P. K. Weber, H. Wang, J. Guo, H. Dai, N-doping of graphene through electrothermal reactions with ammonia, Science 324 (2009) 768-771.

[29] Y. Liu, Y. Chen, L. Tian, R. Hu, Hierarchical porous nitrogen-doped carbon materials derived from one-step carbonization of polyimide for efficient CO_2 adsorption and separation, J. Porous Mater. 24 (2017) 583-589.

[30] L. Shen, J. Wang, G. Xu, H. Li, H. Dou, X. Zhang, $NiCo_2S_4$ nanosheets grown on nitrogen- doped carbon foams as an advanced electrode for supercapacitors, Adv. Energy Mater. 5 (2015) 1400977.

[31] H. Zhang, Y. Zhou, C. Li, S. Chen, L. Liu, S. Liu, H. Yao, H. Hou, Porous nitrogen doped carbon foam with excellent resilience for self-supported oxygen reduction catalyst, Carbon 95 (2015) 388-395.

[32] K. Daeok, K. D. Woo, B. Onur, K. Min- Kyeong, P. Kyriaki, C. Ali, Highly hydrophobic ZIF- 8/carbon nitride foam with hierarchical porosity for oil capture and

chemical fixation of CO_2, Adv. Funct. Mater. 27 (2017) 1700706.

[33] Z. H. Sheng, L. Shao, J. J. Chen, W. J. Bao, F. B. Wang, X. H. Xia, Catalyst-free synthesis of nitrogen-doped graphene via thermal annealing graphite oxide with melamine and its excellent electrocatalysis, ACS Nano 5 (2011) 4350-4358.

[34] Y. Xia, R. Mokaya, Synthesis of ordered mesoporous carbon and nitrogen- doped carbon materials with graphitic pore walls via a simple chemical vapor deposition method, Adv. Mater. 16 (2004) 1553-1558.

[35] J. Chen, J. Xu, S. Zhou, N. Zhao, C. P. Wong, Nitrogen-doped hierarchically porous carbon foam: A free-standing electrode and mechanical support for high-performance supercapacitors, Nano Energy 25 (2016) 193-202.

Figure Captions:

Fig. 1. Schematic representation of the fabrication of porous CNFs/acrylic resin composite.

Fig. 2. XPS spectra of CNFs: (a) wide scan survey; (b) high resolution C 1s spectra; (c) high resolution N 1s spectra.

Fig. 3. Raman spectra of the samples: (a) CNFs, (b) OCNFs, and (c) MCNFs.

Fig. 4. FT-IR spectra of (a) MF foam, (b) CNFs, (c) OCNFs, (d) MCNFs, and (e) CNFs/acrylic resin composite.

Fig. 5. XRD patterns of (a) CNFs, (b) OCNFs, (c) MCNFs, and (d) CNFs/acrylic resin composite.

Fig. 6. N_2 adsorption-desorption isotherms and corresponding pore size distribution curves (inset) of the samples: (a) CNFs, and (b) CNFs/acrylic resin composite.

Fig. 7. SEM images of (a, b) CNFs and (c, d) CNFs/acrylic resin composite.

Fig. 8. Hydrophobicity of the CNFs/acrylic resin composite: (a, b) water and (c, d) toluene contact angle tests.

Fig. 9. Effect of different loading contents of CNFs on the capture capacities of the CNFs/acrylic resin composites.

Fig. 10. The capture capacities of the CNFs/acrylic resin composites.

Fig. 11. The typical toluene (labeled with Sudan III dye) capture experiment by CNFs/acrylic resin composites on the surface of water.

Fig. 12. Regeneration of the CNFs/acrylic resin composites.

Fig. 1. Schematic representation of the fabrication of porous CNFs/acrylic resin composites.

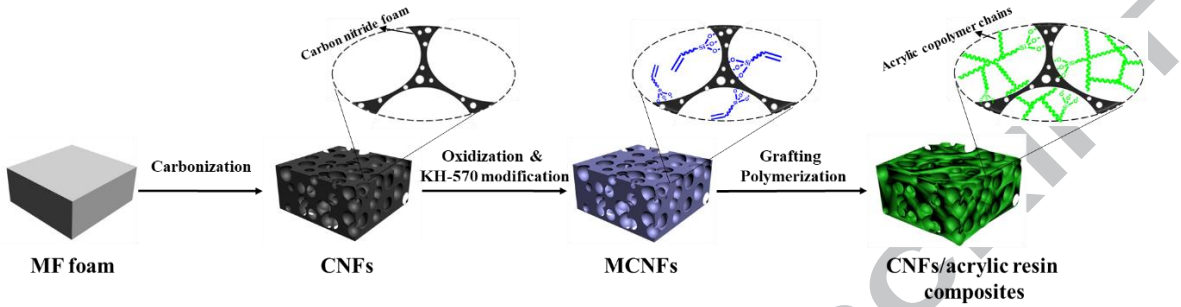

Fig. 2. XPS spectra of CNFs: (A) wide scan survey; (B) high resolution C 1s spectra; (C) high resolution N 1s spectra.

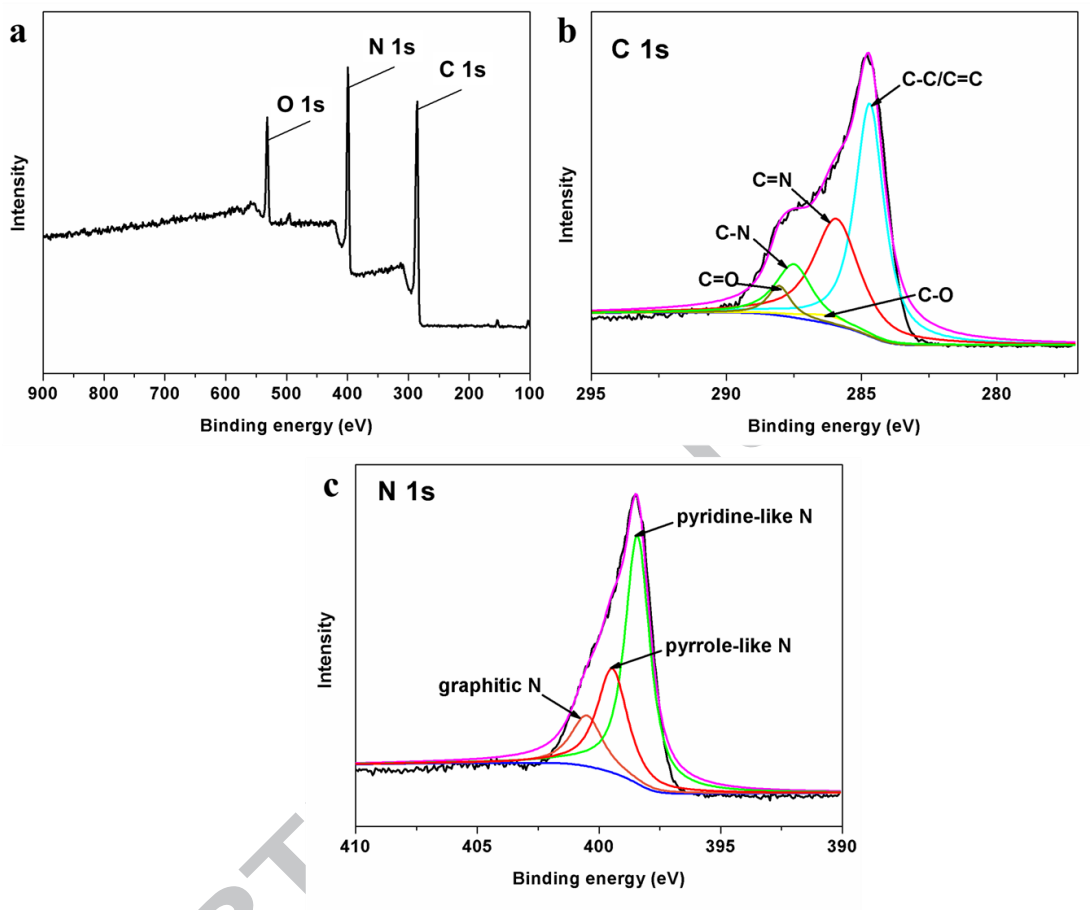

Fig. 3. Raman spectra of the samples: (a) CNFs, (b) OCNFs, and (c) MCNFs.

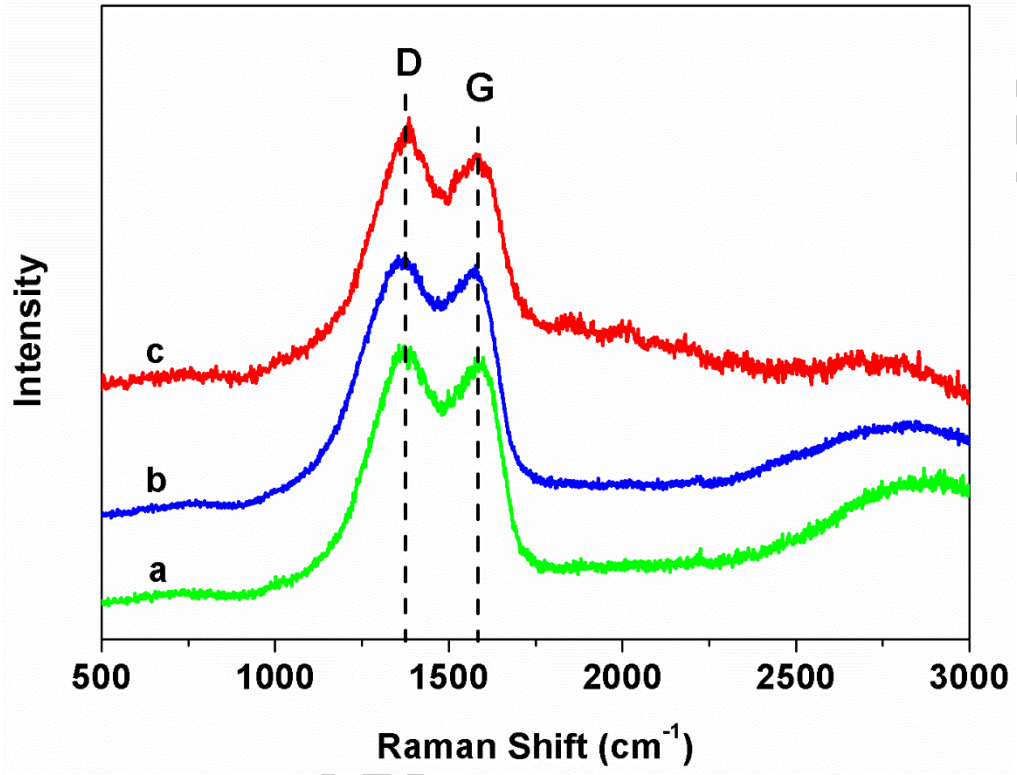

Fig. 4. FT-IR spectra of (a) MF foam, (b) CNFs, (c) OCNFs, (d) MCNFs, and (e) CNFs/acrylic resin composite.

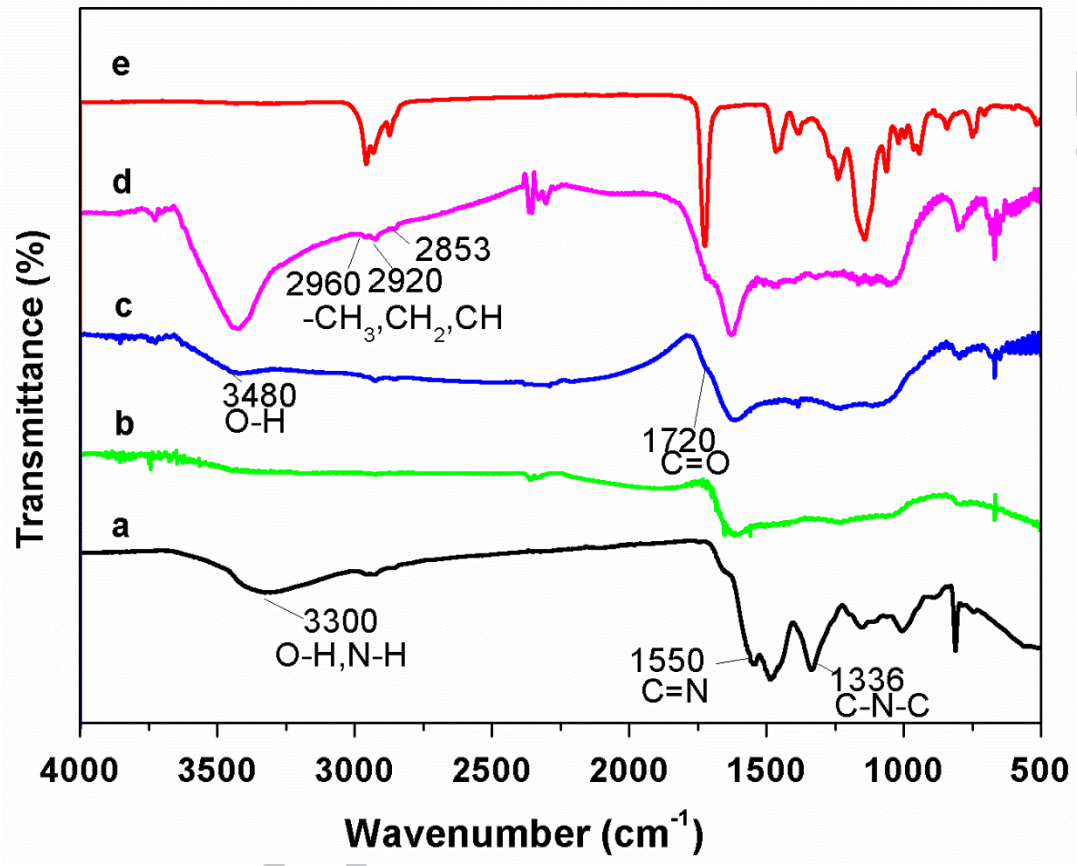

Fig. 5. XRD patterns of (a) CNFs, (b) OCNFs, (c) MCNFs, and (d) CNFs/acrylic resin composite.

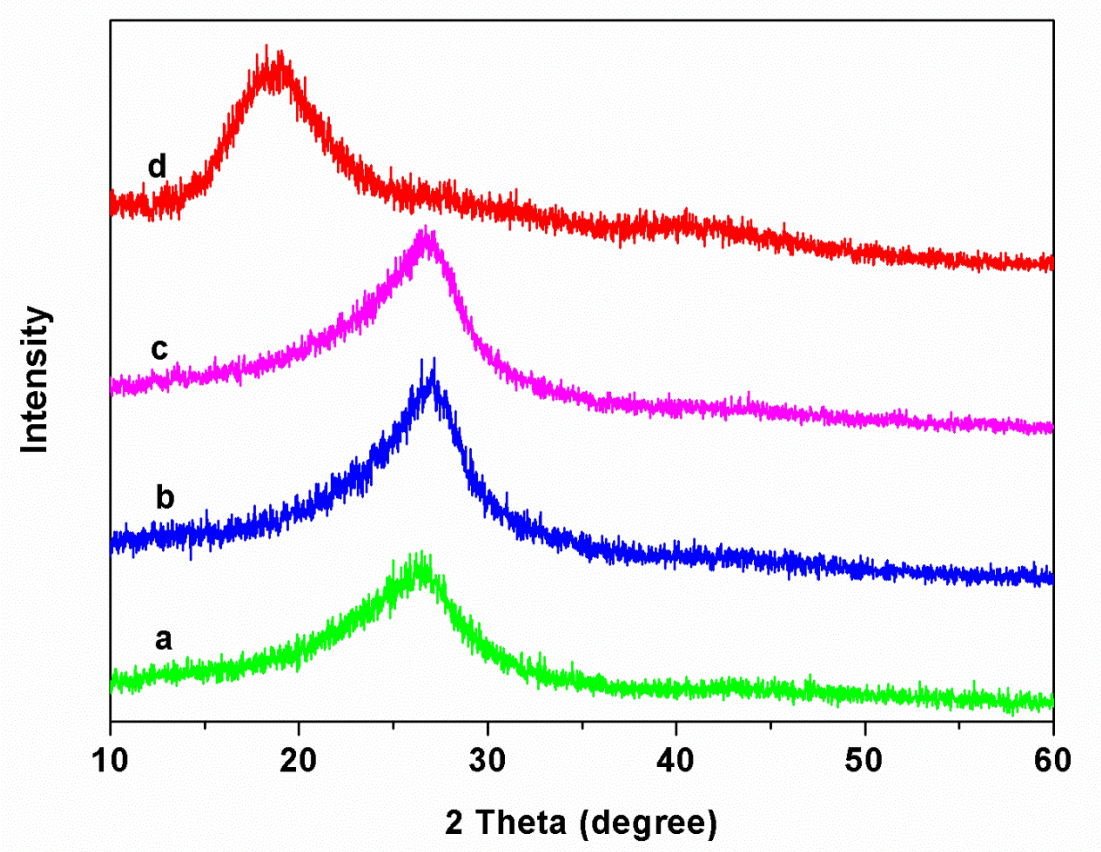

Fig. 6. N_2 adsorption-desorption isotherms and corresponding pore size distribution curves (inset) of the samples: (a) CNFs, and (b) CNFs/acrylic resin composite.

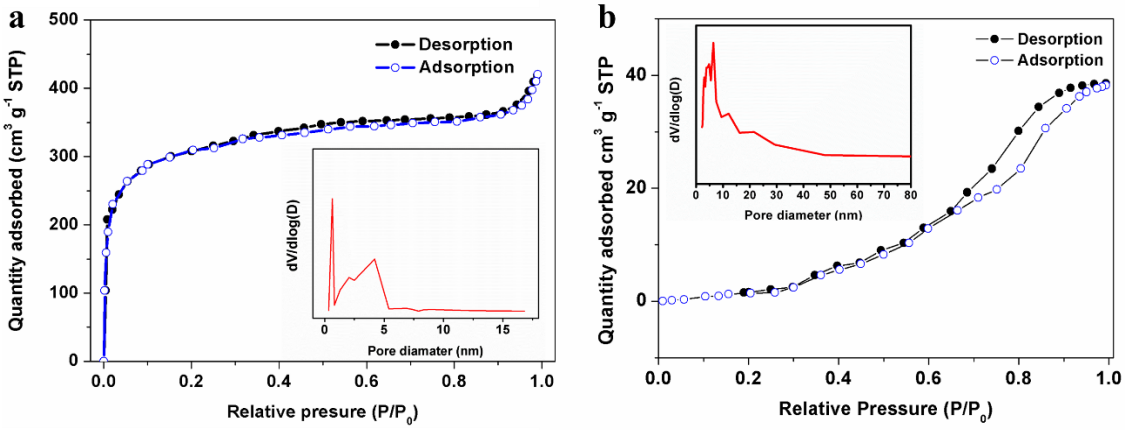

Fig. 7. SEM images of (A, B) CNFs and (C, D) CNFs/acrylic resin composite.

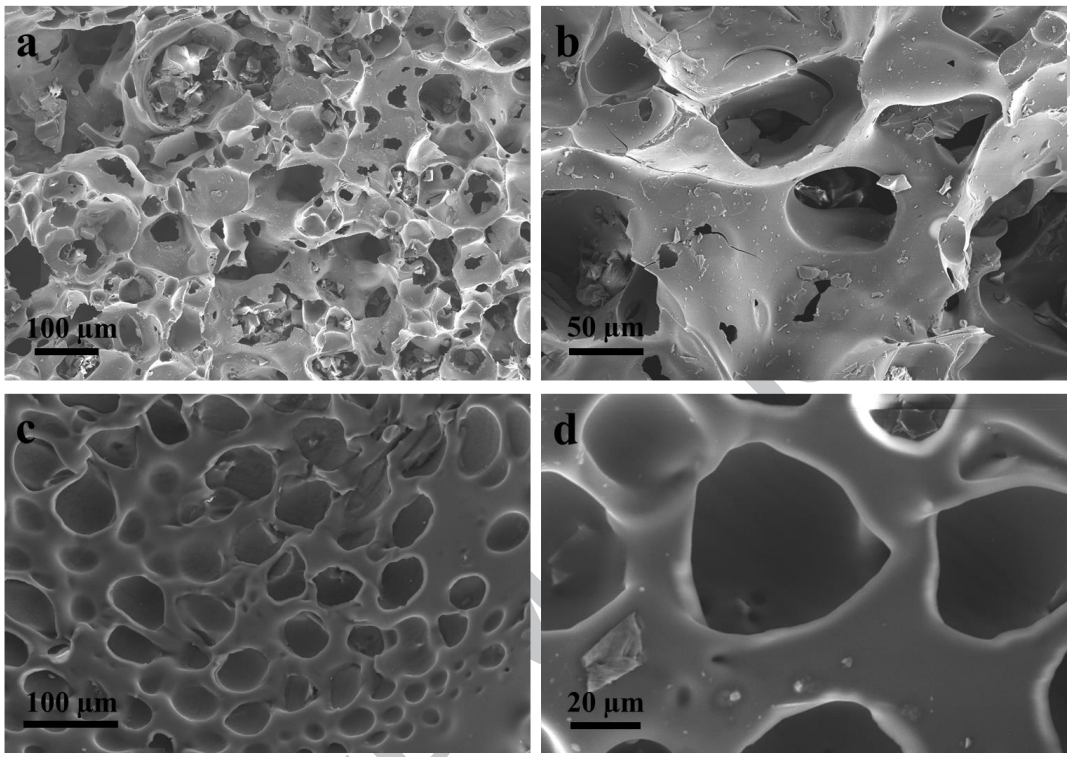

Fig. 8. Hydrophobicity of the CNFs/acrylic resin composite: (A, B) water and (C, D) toluene contact angle tests.

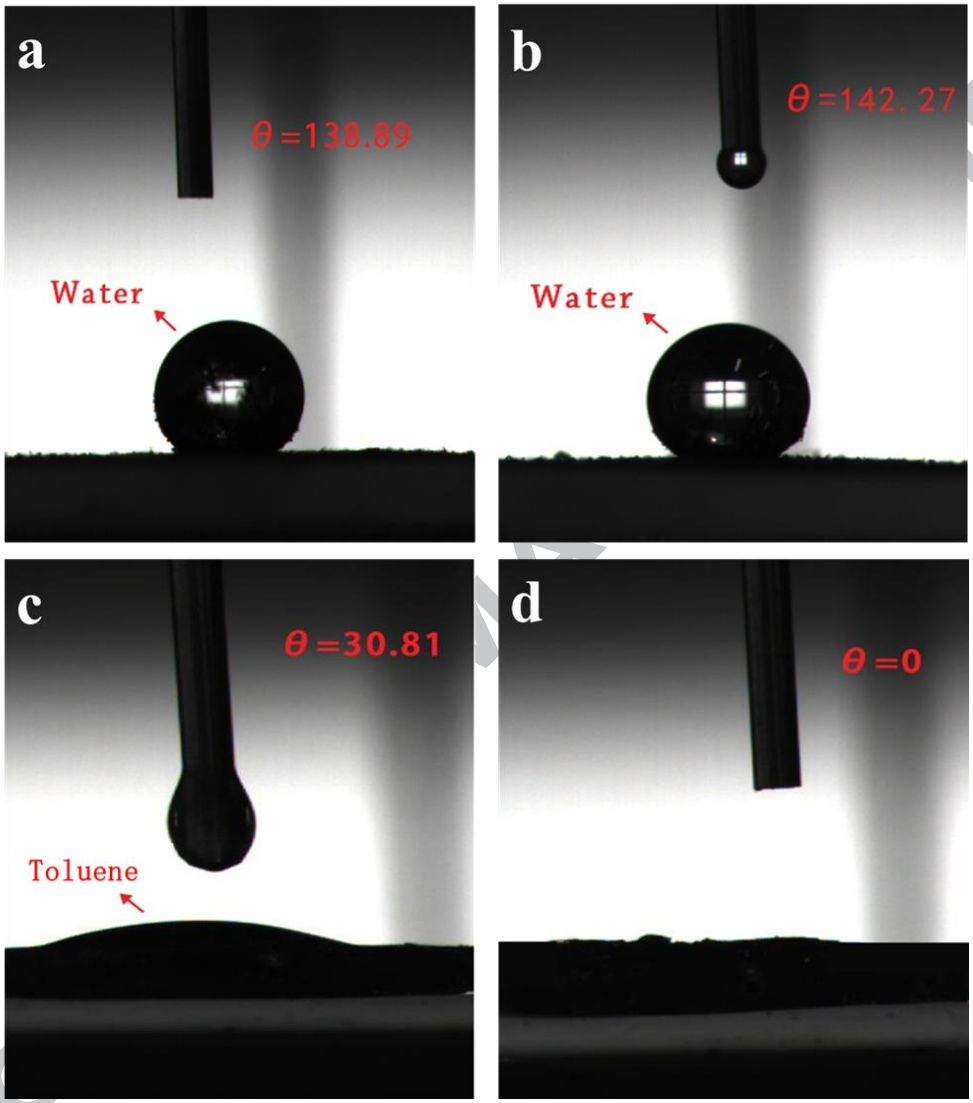

Fig. 9. Effect of different loading contents of CNFs on the capture capacities of the CNFs/acrylic resin composites.

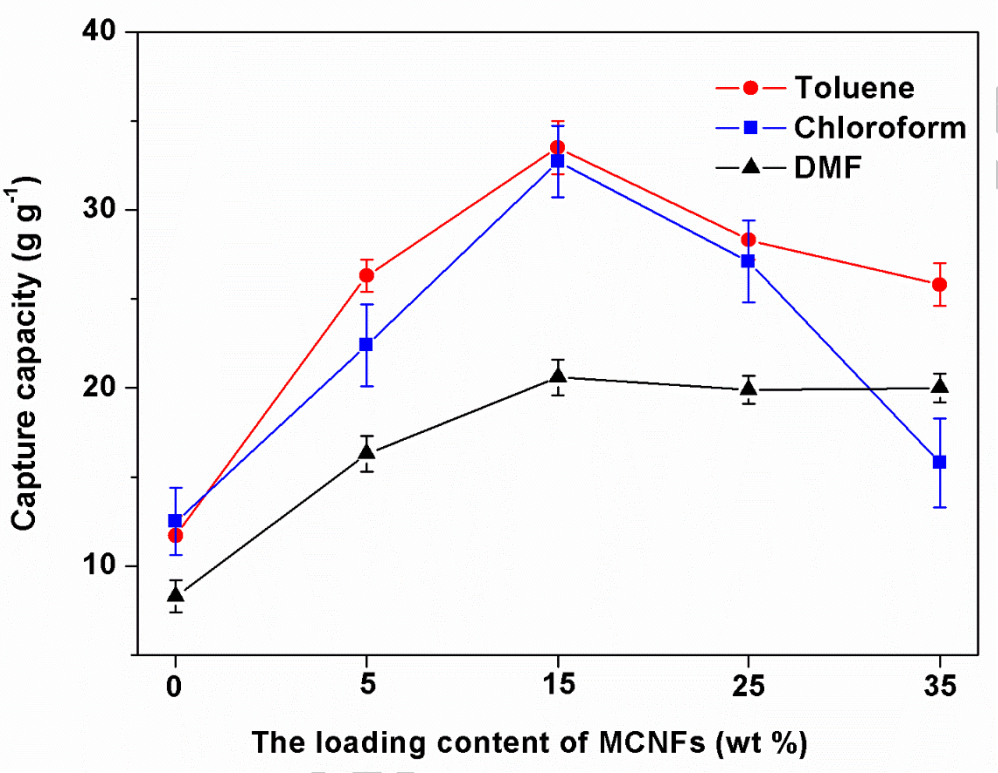

Fig. 10. The capture capacities of the CNFs/acrylic resin composites.

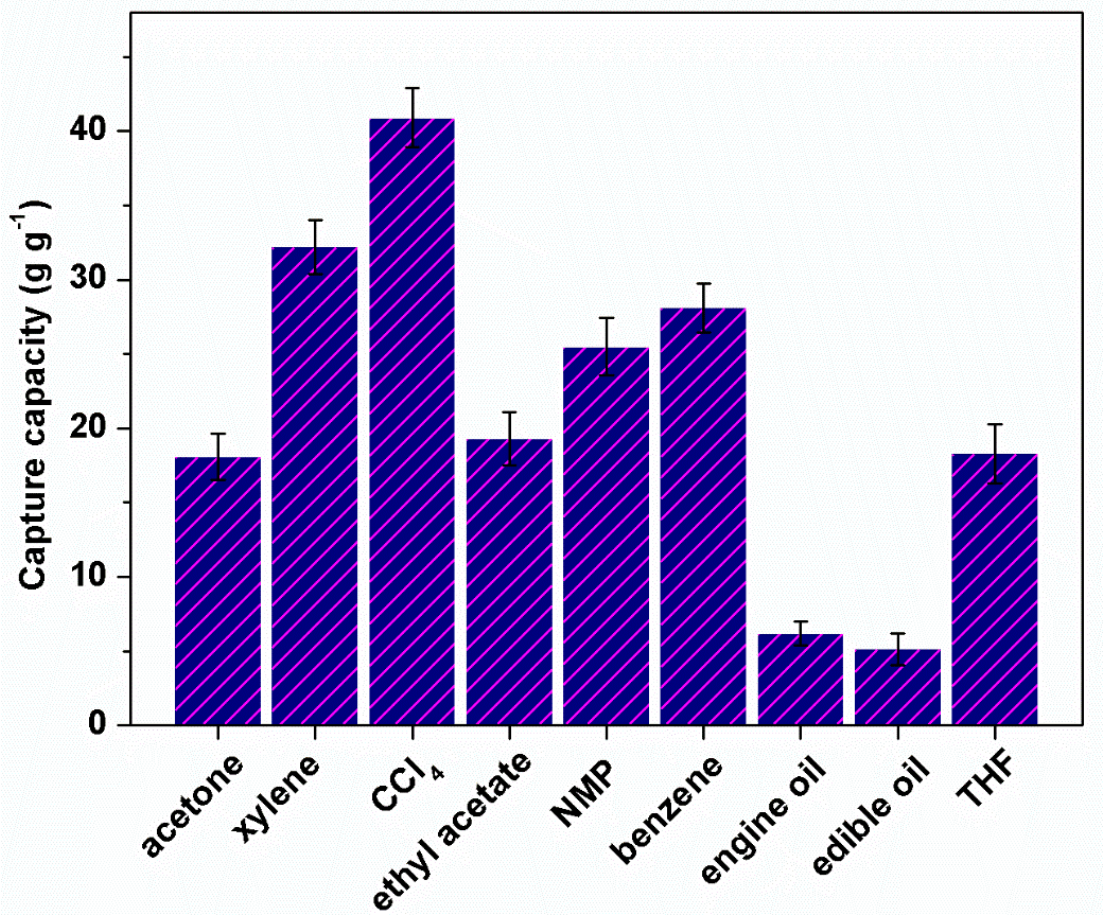

Fig. 11. The typical toluene (labeled with Sudan III dye) capture experiment by CNFs/acrylic resin composites on the surface of water.

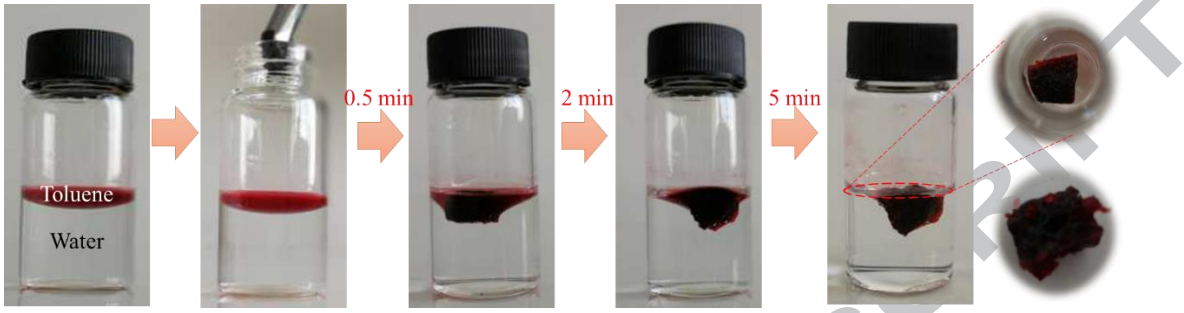

Fig. 12. Regeneration of the CNFs/acrylic resin composites.

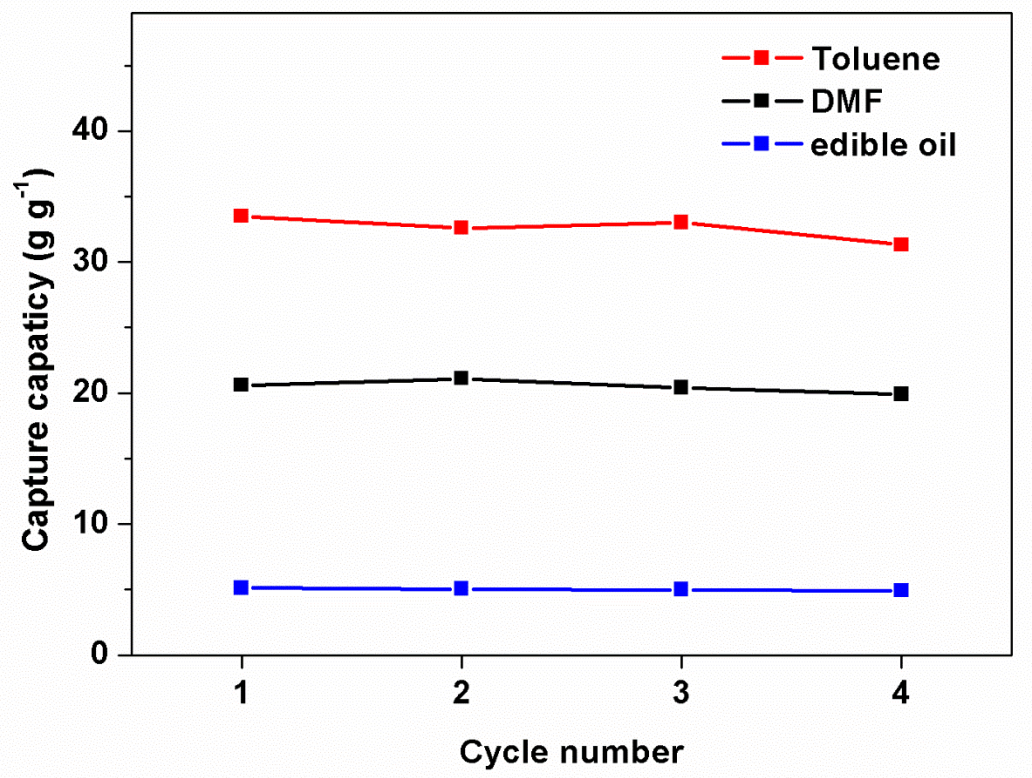

Fabrication of porous carbon nitride foams/acrylic resin composites for efficient oil and organic solvents capture

Highlights:

- CNFs with hierarchal porosity and large specific surface area were synthesized.
- CNFs/acrylic resin composites were fabricated by *in situ* polymerization.
- The composites exhibited a high oil capture capacity (5.1~40.9 g g^{-1}).

Fabrication of porous carbon nitride foams/acrylic resin composites for efficient oil and organic solvents capture

Graphical abstract